Charge Sharing between two adjacent strip electrodes in a CdTe detector induced by the same primary photon: Part I.

Internal Report IASF/BO n. 435/2005
(December 2005)

Authors:
G. Ventura [(1)]
N. Auricchio [(1), (2)]
A. Donati [(1)]
E. Caroli [(1)]
F. Schiavone [(1)]
W. Dusi [(1)]
A. Cola [(3)]
E. Perillo [(4)]
A. Raulo [(4)]

Affiliations:
[(1)] INAF/IASF-Bologna
[(2)] Dipartimento di Fisica, Università di Ferrara
[(3)] IMM CNR-Lecce
[(4)] INFN-Napoli

1. Aims and summary

This document reports the results of the measurements performed with an X-Ray detection system based on a 15 strip CdTe detector coupled to a Front-End readout ASIC from eV products.
The experimental set-up (HW and SW) is described in the text together with the measurements scheme and the raw results. The main objective of the experimental activity consists in quantitative evaluations of the charge collected by two adjacent detector strips induced in a CdTe crystal by the same primary photon. The sense of the expression "charge condivision" or "charge sharing" just refers to the fact that a unique X-Ray event releases in the CdTe detector a charge which is not collected by a single electrode, but rather shared between two adjoining anode strips. Analog data coming from the two selected CdTe anode strips are processed, converted in digital form and flagged in order to distinguish if the events are single hit or double hits, i.e. if a charge packet has been collected by a single strip or if two charge clouds have been separately induced in the two selected strips within the time selected for the coincidence window. The coincidence function is performed by a hardware circuitry while the selection between single and double events is performed by off-line analysis (off-line SW). The experimental set-up simply analizes the signals' energy also giving a code for single or double events and stores raw data without any preliminary analysis which could cause loss of information.

The report is subdivided in two parts. The first part mainly describes the experimental set-up and presents the results obtained with a first approximation analysis on the raw data, while the second one will be dedicated to the description of the off-line SW tools used to extract significative evaluations on the charge sharing events and to the results discussion.

***Applicable Documents*:**

Authors	**Title**
E. Caroli et al.	"***Report sull'analisi preliminare dei dati di H/K dell'esperimento CACTμS: andamento di parte dei dati di housekeeping registrati durante il volo transmediterraneo (luglio 2002)***", RI IASF-Bo, N. 346, 2002
N. Auricchio et al.	"***Descrizione e manuale d'uso dell'elettronica a gamma camera per rivelatori a stato solido segmentati (microstrip pixellati)***", RI IASF-Bo N. 404, 2004
N. Auricchio et al.	***Spectroscopic characterization of a Multipixel Detector in an eV Multi Pix 16 Channel ASIC Evaluation System***", RI IASF-Bo N. 387, 2004
N. Auricchio et al.	*"**eV Multi Pix 16 Channel ASIC Evaluation System**"*, RI IASF-Bo, N. 388, 2004

2. The CdTe detector

On a surface of the 2 mm thick CdTe detector crystal body produced by Eurorad (Strasbourg, France) 15 golden strip electrodes, i.e. anodes, have been metalized by Baltic Scientific Instruments (Riga, Latvia). On the external edge of the anodes' surface a metalized frame (Guard Ring) should act as corrector by reducing the electrical field non-uniformities on the detector borders.

The monocathode, metalized with gold in the opposite surface, is biased at a negative voltage while the anode strips are DC coupled to the inputs of an ASIC eV-16 (15 used). The guard ring is held at 0 V bias. The monocathode surface is exposed to the X-ray beam. **Fig. 1a** shows a section of the detector with some details and geometrical dimensions, **Fig. 1b** the anode strip surface with the guard ring, **Fig. 1c** the arrangement implementing the physical and electrical connections for the bias voltages and the strip output signals.

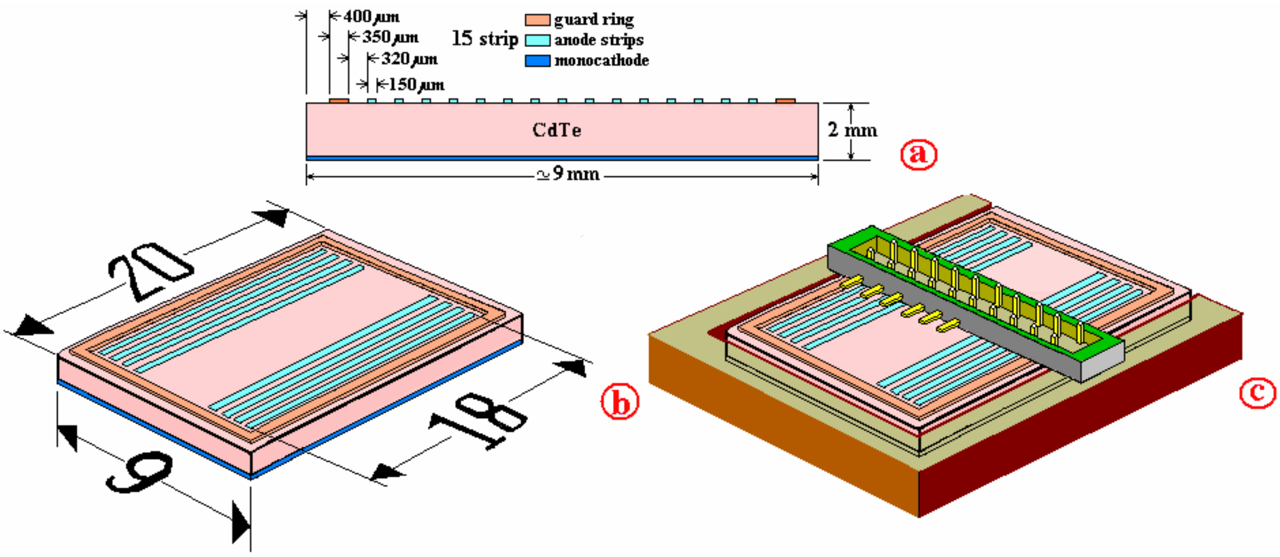

Fig. 1. The CdTe detector with 15 anode strips: **a)** cross section showing the dimensions of the electrodes, **b)** external dimensions in mm of the detector body with the anode strips in evidence, **c)** I/O connector for the bias and the links of the anode strips to the ASIC inputs; the wirings between the anode strips and the I/O connector terminals (20 pins distributed on two rows) are accomplished by gold bondings.

3. The detection equipment and the measurement Set-Up

The detection equipment is schematically shown in **Fig. 2**. The X-Ray source, dipped in a plastic cylinder, can be coupled to two basic collimators assemblies for the main configurations used in the measurements. In the configuration of **Fig. 1a)** the X-ray source, glued in its plastic container, can be precisely inserted in a PVC cylinder which, in turn, is mechanically fixed to the main mechanical assembly sustaining the tungsten (W) collimator. The main mechanical assembly can run on two rails connected to the anti-vibration plane in order to to allow possible adjustements without loosing the overall alignment. The CdTe and Front-End Electronics Box (CdTe/FE Box) is faced to the W plane on which the rectangular collimator lid is constructed, i.e. the effective X-Ray emitting area. The distance between the W plane and the CdTe/FE Box entrance window is limited to a few tenths of microns, while the distance between the CdTe/FE Box entrance window and the detector cathode plane is about 8 mm. The CdTE/FE Box, rigidly fastened to motorized tables, can be independently moved in horizontal or in vertical directions with a position resolution of the order of 1-2 microns, allowing to irradiate different areas on the detector surface. This mechanical set-up permits to collect data in the "scanning" mode, i.e. to accumulate data when different and pre-selected detector areas are exposed, or at fixed positions.

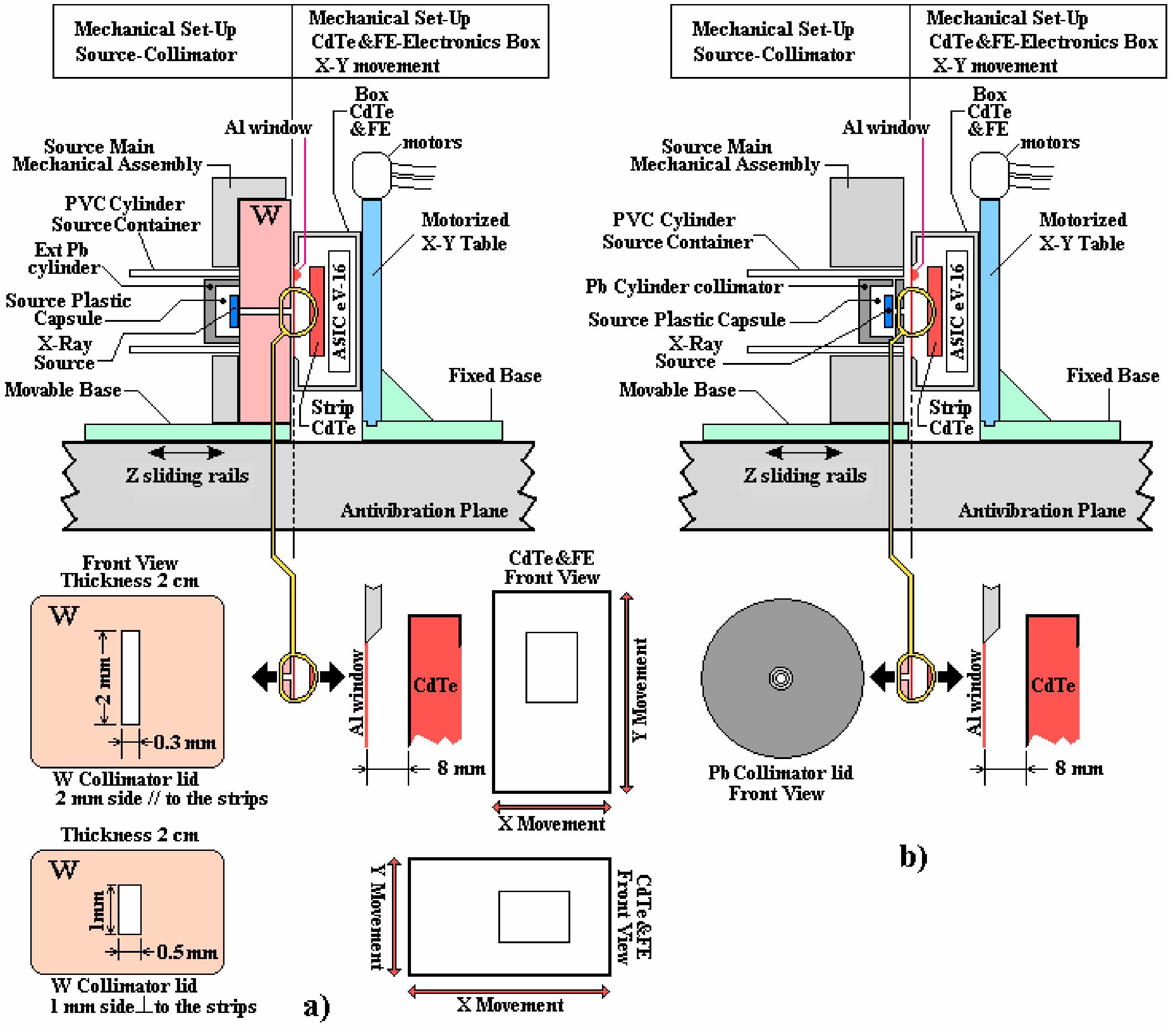

Fig. 2. Two possible configurations of the detection equipment. **a)** Detection assembly with collimated X-ray source permitting precise positioning of the CdTe/F Box by acting on the X-Y motorized tables. This configuration is used for the measurements in "scanning" modes. **b)** Detection assembly with partly collimated X-ray source and the CdTe/FE Box in a fixed position. This configuration, used for the wide angle illumination exposures, allows three collimator's apertures, i.e. three diameters of the output lid of the Pb collimator, which permits an almost uniform distribution of the X-ray source intensity at the CdTe. Possible diameters are 3 mm, 2 mm and 1.5 mm.

The overall distance from the X-Ray source and the CdTe detector plane is then 2 cm + 0.8 cm ≅ 2.8 cm. Two different W lids have been used in the measurements. The first one, with dimensions of 0.3mmX2mm being the 2 mm side parallel to the anode strips, gave an effective cathode surface illumination of 0.56mmX3.76mm; the second one, with dimensions of 0.5mmX1mm being the 1 mm side ortogonal to the anode strips, illuminated an effective cathode area of 0.9mmX1.8mm. The relative positioning of the higher dimension of the collimator lid with respect to the anode strips (i.e. parallel or orthogonal) is described in some details later and depicted in **Fig. 7** and **Fig. 8**, respectively. So strong levels of collimation require quite long accumulation times in order to have significant statistics and, at the same time, is far from delivering a point-like spot on the detector surface. **Fig. 2b)** shows the experimental arrangement for the data collection not requiring precise positioning (the positions X_B and Y_B of the CdTe/FE Box are fixed) and also wide aperture collimation apertures. Most of the mechanical features are similar to those relative to the scanning mode as can be seen from a comparison between **Fig. 2a)** and **Fig. 2b)**. Three Pb collimator apertures can be used (1.5 mm, 2mm, 3 mm) in order to partly equalize the X-Ray beam intensity at the detector to the actual natural activity of the emitting source. This configuration is used for data accumulations for almost open X-ray source.

The picture of **Fig. 3** shows the HW assembly arranged for the CdTe detector (**Fig. 1**) and the readout ASIC used for the front end analog data processing (ASIC eV-16).

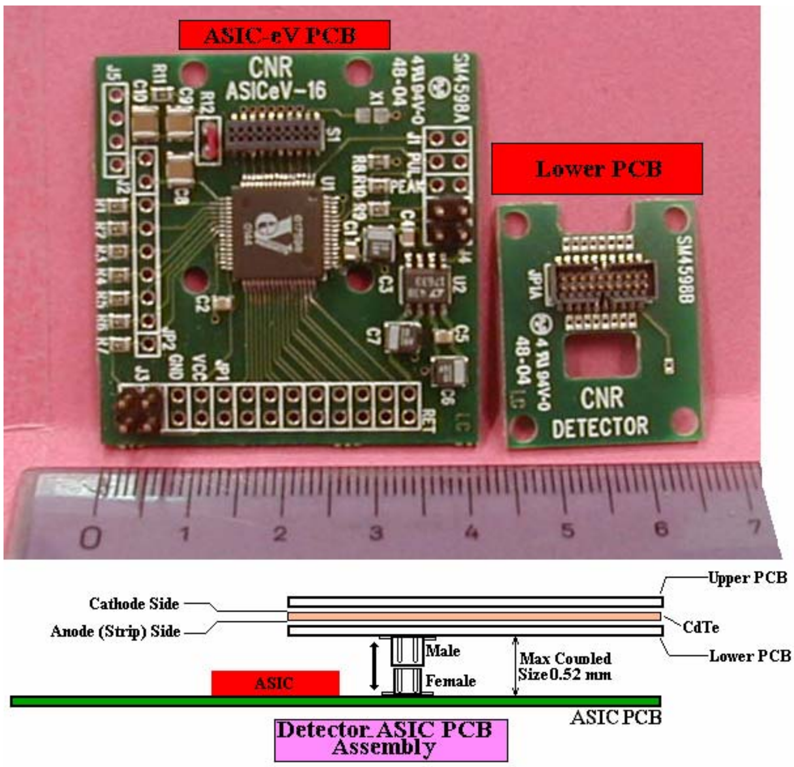

Fig. 3. Printed circuit boards for the ASIC eV-16 (top left side) and for the I/O detector connector (top right side). In the lower part of the picture it is sketched the connection between the CdTe detector and the ASIC PCB.

The two PCBs are coupled together as indicated in the lower part of **Fig. 3** and also explained in the caption of **Fig. 1**. Both the PCBs are wired inside the light-tight CdTe-FE Box coupled to the moving mechanical tables. With the adopted configurations, the cathode surface is exposed to the X-Ray beam. The CdTe/FE Box is connected to the external world as indicated in **Fig. 4**. Analog pre-processed amplified signals are wired to the connector **J1** and then fed to a distribution board housing multiple BNC connectors. Individual pre-shaped signals are enabled to be extracted from the distribution board by coaxial cables from which they can be inserted into the external Read Out electronics (Takes) as shown in **Fig. 5**.

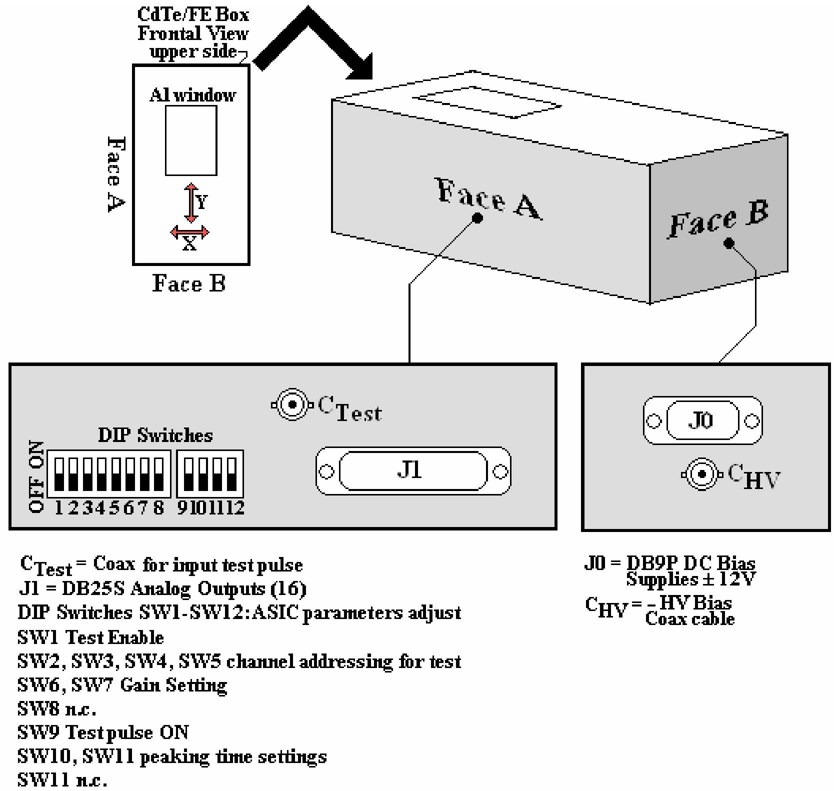

Fig. 4.Schematic view and Input/Output of the CdTe/FE Box.
SW6 & SW7 switch settings for a gain of 200 mV/fC or 100 mV/fC.
SW10 & SW11 switch settings for peaking times (possible values are 0.75, 1.2, 2.0, 4.0 μs).

4. Set-up HW for data-processing and acquisition

For two adjacent detection channels the HW set-up is shown **Fig. 5**.
The Takes electronics can process a set of up to 16 analog channels provided by solid state detectors. Since the Takes internal amplification factor is set at too high values for the ASIC eV-16 output levels, it is necessary to lower the overall amplification factor by using series resistors on any measurement channel (R = 15 kΩ, Gain Adjust in **Fig. 5**). Furthermore, the AC coupling of the Takes electronics' input channels ensures for the elimination of the DC offset provided by any ASIC eV output channel. The signals from the two adjacent strips selected for the measurements are fed to the Takes electronics by coaxial cables and analogically processed with the following rule: any signal is presented to a peak stretcher (**PPS**) and to a voltage comparator (minimum energy threshold $\mathbf{E_{min}}$). The peak voltage of any analog signal overcoming $\mathbf{E_{min}}$ is pre-stretched for a time of the order of the input pulse rise time. For the two-strip signals configuration if within the coincidence window time, selectable among 1, 2, 4, 8, 16 μsec, the two digitized outputs coming from the energy thresholds $\mathbf{E_{min}}$ occur, a post stretching action is issued and the analog data are enabled to be converted in digital by the analog-to-digital converter (ADC). In the present experiment the coincidence criterion is simply based on the fact that single or double events

detected within the coincidence time (selectable among 1, 2, 4, 8, 16 μsec) are accepted as valid and then post-stretched to be converted in digital by the 12 bit flash ADC.

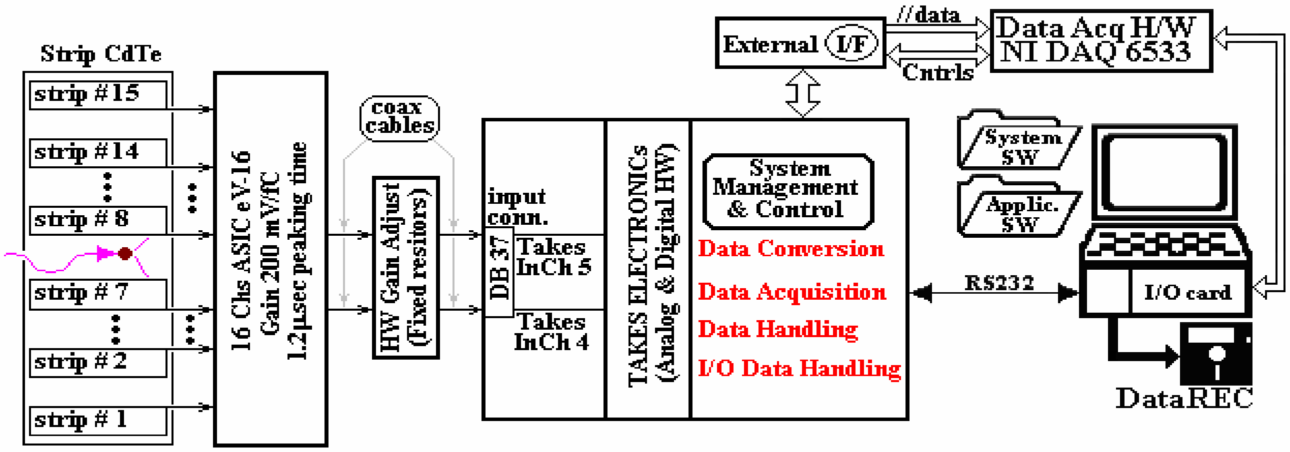

Fig. 5. Experimental set-up to extract information on the signals with charge shared by two adjacent strips, i.e. events induced in the CdTe detector by an individual primary X-Ray.

In the experimental set-up of **Fig. 5**, which refers to two signals handling, the energy of any event (single or double overcoming $\mathbf{E_{min}}$) is coded with 10 significant bits and to any channel an address code is associated. Takes also adds a coded field which allows to detect if a single or double event has occurred within the selected coincidence time.

Takes reserves a word of 32 bit to any single event, two 32 bit pattern for any double event. Furthermore, for design reasons, Takes provides output coded data in serial form.

The energy, address and event type coding are shown in **Fig. 6**: any event is represented by a 32 bit data, which means that an output 32 bit data is provided for single events while two events in coincidence are outputted as two 32 bit data.

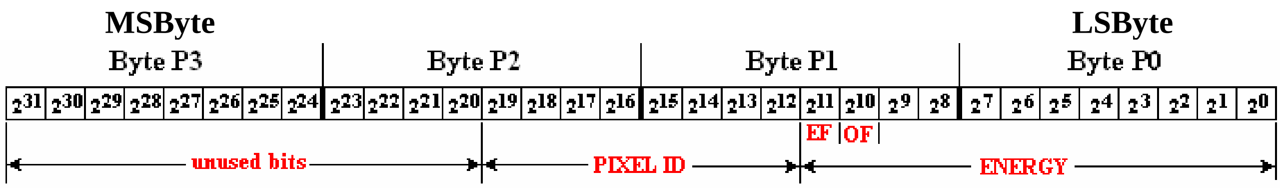

Fig. 6. Event Coding.

Energy: Signal amplitude coded with 10 bit resolution (1024 energy channels). The two LSBits of the ADC are not used.

OF: Overflow flag; if OF=1 the signal is over the maximum energy threshold.

EF: End-of-event; if EF=0 a single channel has been excited, if EF=1 a double event has occurred.

PIXEL ID: Excited CdTe address with 8 bit resolution.

The external data acquisition is based on a National Instruments digital interface NI DAQ 6533 which handles the parallel data transmission to the central PC. The Takes output serial data required an HW conversion in parallel form (External I/F in **Fig. 5**) to be acquired by the NI DAQ 6533.

The SW modules, written “ad hoc” in the National LabView environment, are:

- Acquisition SW overheading the data-collection and the handshaking between Takes and the I/F NI DAQ 6533 (Flag and Data Acknowledge);
- SW for the raw data storage in files;
- Quick-look management during the data acquisition;
- SW for the Takes initial parameters settings (remote commands through the RS232 link in **Fig. 5**).

5. Data selection for the extraction of the double-charge sharing events

The objectives of the experiment consist in considering the charge detected by the two adjacent strips in the CdTe bulk by a single primary photon, i.e. double event charge signals collected by two independent detector strips within the coincidence window. To measure this effect the region between the strips (intermediate gap) shall be irradiated by a radioactive source. Due to the dimension of the gap, a high precision motion control with a strongly collimated X-Ray spot (ideally, it should be required a point-like X-Ray spot irradiating the detector gap) is needed to be sure to expose the desired region.

However, since the available radioactive source activities are not too high and the collimator dimensions set a limit to reasonable accumulation times combined with the fact that it is almost impracticable to excite a detector region strictly limited to the inter-strip gap, problems can arise to collect reliable data statistically significant. In the laboratory set-up the finite dimension of the spot has geometrical dimensions higher than the intergap distance, implying that double charge condivision events are mixed with other double-type events. In other words, the combination of the too large physical dimensions of the irradiated detector areas and the limited Gamma-Ray source activities have the consequence that signals in coincidence within the window set for the measurements are not all due to charge condivision events, but can be originated by different interaction mechanisms. In particular, data enabled as valid by the coincidence circuit, not always satisfies the main charge sharing criteria, in the sense that they can be considered by the acquisition system as acceptable, but are false from the point of view the charge condivision: e.g. two different primary photons contemporary impinging on the two adjacent strips inside the coincidence window time are considered as double event by the HW coincidence circuit but they are not charge condivision events. In conclusion, the main drawback is represented by the fact that the coincidence HW circuit does not permit to directly distinguish between charge condivision events, induced by a single primary photon, and double events, produced by two coincident primary photons or other double events. Off-line analysis on collected data can permit to partly isolate the charge-shared data from undesired coincident ones: unwanted data are rejected by SW off-line action guided by the physical considerations just described and with the decision criteria described later. Since the probability of false events increases with the coincidence time, to increase the percentage of true charge condivision events is preferable to use coincidence times as lowest as possible, i.e. of the order of the signal peaking time. Furthermore, in order to avoid that primary photons, originated by multiple energy emission sources, could make more difficult to extract the charge sharing events, most measurements have been performed with semi-open sources (mainly ^{57}Co with a cylinder collimator of 1.5 mm diameter) since a unique energy (122 keV) is delivered to the detector.

6. Measurements' programming and preliminary results

The adjacent strips # 7 and # 8 have been chosen as most qualified for the sharing charge condivision tests since they are placed in the central part of the CdTe detector and then should be less sensible to possible effects due to the electrical field non uniformities near the external sides of the detector body. **Fig. 7** shows the three main geometrical arrangements adopted for the tests: **a)** refers to the horizontal (0X) scanning set-up with the X-ray source collimated by the 0.3mmx2mm W lid, **b)** the CdTe/FE Box is held at a fixed position and semi-open source exposition is obtained by Pb cylindrical collimators, **c)** vertical (0Y) scanning set-up with the X-ray source collimated by the 0.5mmx1mm W lid.

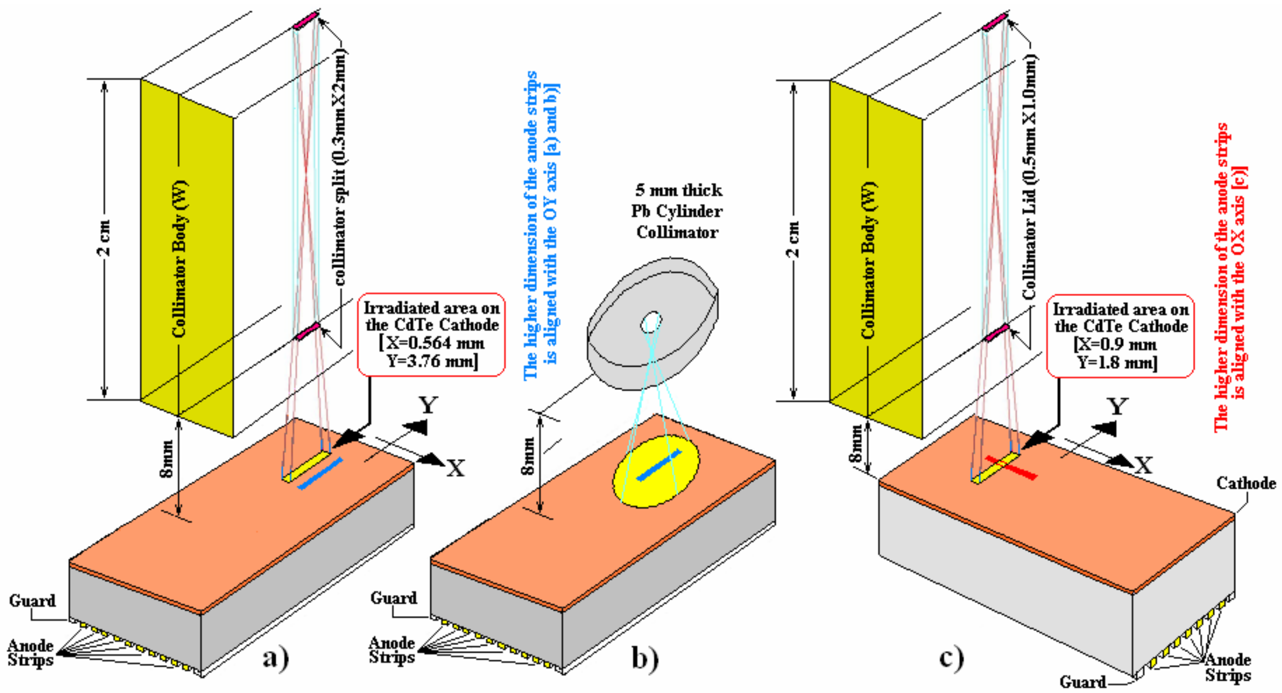

Fig. 7. Main experimental set-ups with some geometrical parameters in evidence.
a) arrangement for the 0X scanning measurements with collimated X-Ray source (**W** collimator **A,** lid with x=0.3mm, y=2mm). Anode strips parallel to the 0Y axis; **b)** at a fixed detector position and partly collimated X-Ray source (Pb collimators **B**, **C**, **D**, with 3 mm, 2 mm, 1.5 mm diameter, respectively); **c)** 0Y scanning measurements with collimated X-Ray source (**W** collimator **E,** lid with x=0.5mm, y=1mm). Anode strips normal to the 0Y axis and CdTe/FE Box rotated by 90° with respect to the arrangements of **a)** and **b)**.

The dependence of the charge sharing on the CdTe bias supply has also been investigated at three different values of the cathode voltage (–75V, –100V, –125V). For all the measurements the guard is kept at 0V bias.

In normal measurement conditions the strip # 7 is connected to the Takes input Ch 4 (**Fig. 5**) and the strip # 8 to Ch 5. To investigate for possible non-uniformities of the Takes analog processing channels, two tests have been performed by exchanging the inputs, i.e. strip # 7 to Ch 5 and strip # 8 to Ch 4 (Strip Exchanged file). Significative non-uniformities were not detected.

The configurations adopted to irradiate and possibly extract the charge shared events (**Fig. 7a** and **7 b)**) have the drawback that, since a point-like X-Ray spot at the detector is almost impossible, the extended irradiated surface involves significant amounts of detector active areas and several events may occur in the preset coincidence window. As a consequence other interactions may be detected which can be confused as charge shared events. **Fig 8** shows the effective cathode areas irradiated by the X-Ray source corresponding to the three set-ups represented in **Fig. 7a), 7b), 7c)** and, as they could appear in transparency, the illuminated anode strips. By the collimation set-up of **Fig. 7c)** we have tried to avoid to collect events mistakable as charge shared, as for example those events which, induced by independent photons directly impinging on the two strips within the coincidence window, deliver the full primary photon energy. The criterion consists in using a collimator assembly which permits a limited control of the CdTe irradiated area, possibly preventing from illuminating both the detector strips at the same time as shown in **Fig. 8c)**.

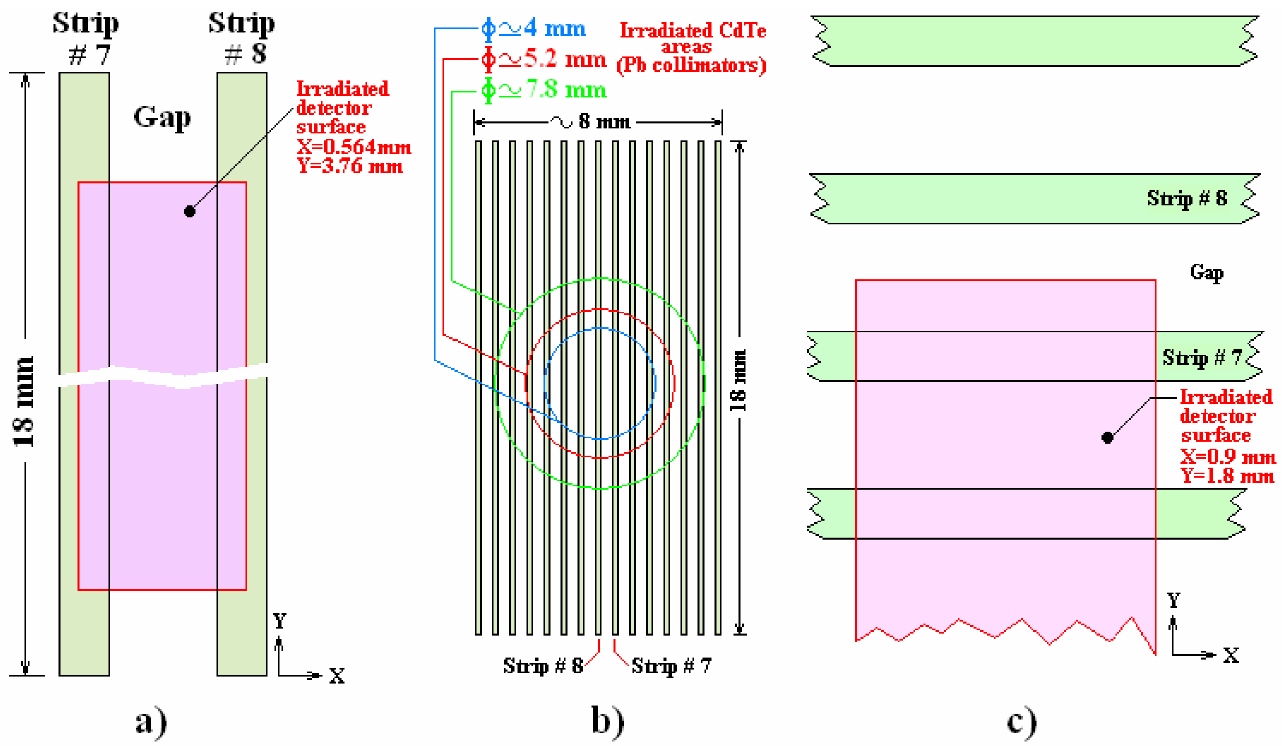

Fig. 8. Sketches of the three CdTe cathode irradiation configurations corresponding to the set-ups of Fig. 7 (the geometrical scales are not respected). The detector areas irradiated are viewed from the cathode surface together with the anode strips 7&8 in transparency. **a)** Detector illuminated area with the W collimator lid of 0.5mmx2mm parallel to the strip [Fig. 7a)]. Scannings in 0X direction at a fixed Y. **b)** Illuminated areas by using the Pb cylinder collimators of Fig. 7b). Tests at fixed X and Y positions. **c)** Expected irradiated area following to a 90° CdTe/FE Box rotation with respect to the arrangement of Figures 7a) and b). Scanning in the 0Y direction at a fixed X.

Prior to execute the routine measurements in the scanning modes (**Fig 8a and c**), it was necessary to find a position reference or to approximately “center” a strip with the X-Ray spot, which was obtained with the following procedure. By acting with the motorized tables in the 0X direction for the set-up of **Fig. 8a)** and in the 0Y direction for the case of **Fig. 8b)**, the integral counts at the X-Ray source main energy peak were recorded as a function of the displacement. The coordinates X_C and Y_C at which the integral counts reach the maximum values correspond to the “zero” or “pixel center” in the X- and Y-scanning modes, respectively. Thereafter, the scanning movements in 0X and 0Y are referred to these coordinates. In more details, the alignment with a strip assumed as a reference, i.e. the strip # 7, has been obtained by irradiating the CdTe with a ^{109}Cd source and then reading the integral counts at the 22-26 keV peak of the processed signals from both the strip 7 and 8. The results of the centring operations are reported in **Fig. 9** for the scanning in the 0X direction, in **Fig. 10** for the 0Y direction. This test gave the reference coordinates [X_C or Y_C] from which issuing the movements to reach the desired positions during the storage of the measurements. **Fig. 9** and **10** show the normalized illuminations of the strip # 7 and # 8 at several X and Y positions, depending on the scanning set-up. Mainly for the movement in the 0Y direction it is clearly shown that there are positions, even if not sharply defined, for which only one strip is illuminated while the other is totally unexcited. The three vertical bars in **Fig. 10** indicate the three positions at which data were accumulated for 21600 sec (6 hours).

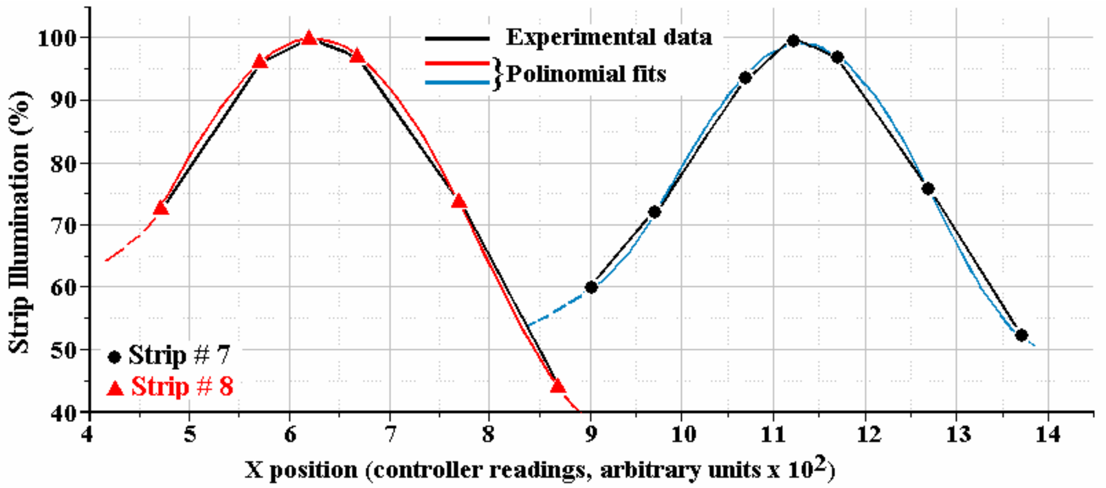

Fig 9. Normalized strip illuminations as a function of the position X. The gap is not well definable when scannings in the 0X direction are performed, since the X-Ray spot tends to involve both the strip 7 and 8 at the same time.

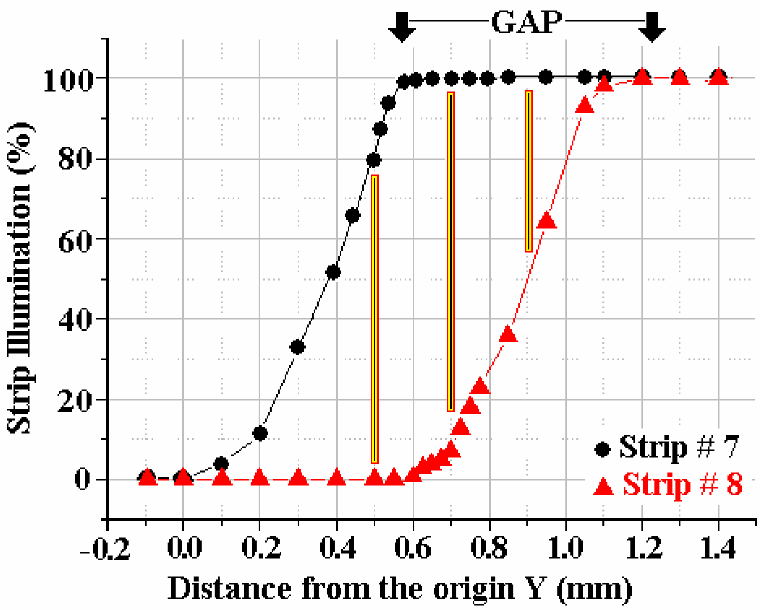

Fig. 10. Normalized strip illuminations as a function of the position Y. The vertical lines indicate the coordinates at which the measurements have been performed and an evaluation of the detected gap is also given.

6.1. Scanning tests

6.1.1. The X-scanning has been performed at a vertical fixed position (Y=12000 motor controller units, approximately corresponding to the alignment of the baricenter of the X-Ray spot with the center of the CdTe detector) and X variable. At any X position the CdTe was irradiated by a collimated ^{109}Cd source (**Fig. 7a**). The main limit of the test is represented by the fact that the horizontal dimension of the irradiated detector area (~0.56 mm) is higher than the gap dimension (~ 0.32 mm) and then the expositions can involve two adjacent strips at the same time (see, for example, **Fig. 8a**). This implies that is quite improbable to excite a single strip or an intermediate location without interfering with the other strip. In other words the available collimator lid irradiates a detector surface which involves too large CdTe areas to be sure to excite only the gap. This prevents to be sure that the experimental set-up permits to precisely investigate the region between two adjacent strips without directly exciting both the strips. The result is that, unless of tolerating impracticable exposition times with iper-collimated X-Ray sources, a scanning procedure can give an idea of the behaviour of the double-charge-sharing events. Furthermore, single events directly impinging the strips due to two independent primary photons and occurring within the coincidence accepting time are stored as double events thus giving a false contribution to the double charge sharing events evaluation. In the 0X-scanning mode only the most active X-ray source has been used (^{109}Cd), whose intensity permitted reasonable acquisition times in conjunction with the narrow available W collimator. As measurements starting coordinate it has been assumed an abscissa $X_C-\delta X$ far from a side of the strip # 7 so as the strip # 8 is almost totally unexposed. Data were accumulated for times of 3 h for any X position spaced from the other by 150 μm [files **Cd(i)collim_1us, Appendix II**]. **Table I** summarizes the data collected in the scanning tests.

Table I: summary of the results of the "X" scanning tests; accumulation time=10800 sec (3h).

Position X(mm)	Total Events N_T (Counts)	Single Events (Counts)	Single Events (%)	Double Events (counts)	Raw Double Events (%)
0.15	1687094	1685178	99.89	1916	0.11
0.3	1928507	1913117	99.20	15390	0.80
0.45	1810260	1786513	98.69	23747	1.31
0.6	1846120	1823216	98.76	22904	1.24
0.65	1913900	1893773	98.95	20127	1.05
0.75	2089567	2080179	99.55	9388	0.45
0.9	1607378	1605789	99.90	1589	0.10

Data N_T listed in **Table I** are represented in **Fig. 10,** while the percentages relative to the single and all the double events (i.e. the events expected to be charge sharing due to a unique X-Ray primary photon also including the double events due to different photons as explained in § **5**) are shown in **Fig. 11a)** e **11b)**.

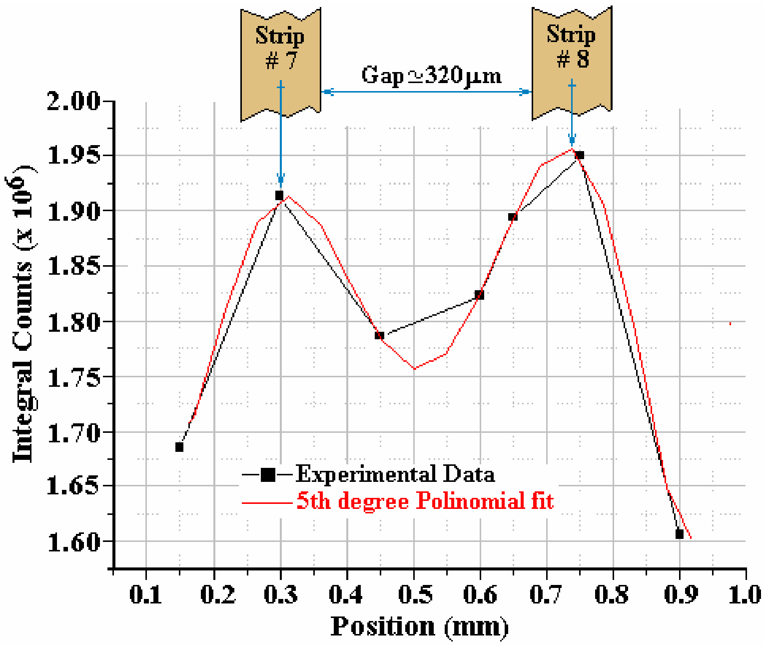

Fig. 10. Behaviour of the integral counts as a function of the horizontal CdTe displacement with a ^{109}Cd emitting source. The scanning has been executed with steps of 0.15 mm with the collimator shown in Fig. 7a. In the upper part the strip dimensions and positions are schematically indicated as detected during the measurements.

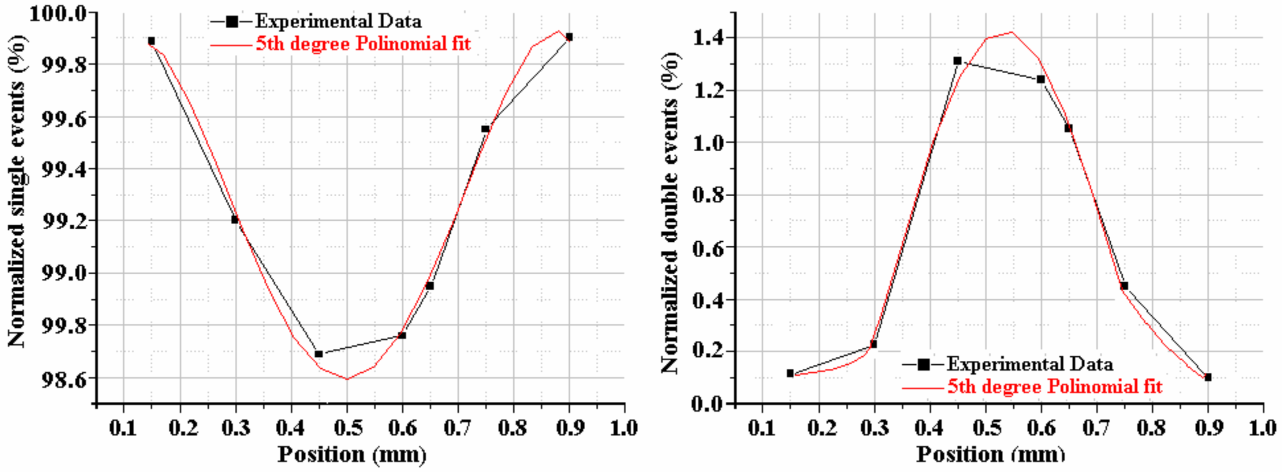

Fig. 11. Detected behaviour of the fractions of single events **[a)]** and of the double events **[b)]** as a function of the horizontal displacement. At any position, homogeneous experimental data are evaluated with respect to the integral counts accumulated.

The movement from a strip to the adjacent seems to produce in the double event percentage an increment of about + 0.05%/μm in the race towards the center of the gap, a decrement of about –0.05%/μm from the center of the gap to the other side strip.

6.1.2. The Y-scanning has been performed at an X fixed (X=8000 motor controller units, roughly corresponding to the alignment of the baricenter of the X-Ray spot with the center of the CdTe detector) and Y variable. At any Y position the CdTe was irradiated with collimated ^{109}Cd and ^{57}Co sources (**Fig. 7c**). The CdTe/FE Box, rotated by 90° with respect to the X-scanning set-up, has been moved to three Y positions indicated in **Fig. 9b)** where data were accumulated for 21600 sec. The long accumulation times were dictated by the reduced irradiated CdTe area due to both the collimator window (0.5mmX1mm) and the illumination of the strips (see **Fig. 8c**). Data were accumulated for times of 3 h at any X position spaced from the other by 150 μm [files **Cα(Yi)_coll_CdTeOrizz_1us, Appendix II**], Cα=Cd or Co, i=Y1,Y2,Y3. **Table II** summarizes the data collected in the scanning tests.

Table II: summary of the raw data results of the "Y" scanning tests; accumulation time=3h. The measurements were performed at the positions indicated in Fig. 10.

Source	Position X(mm)	Total Events N_T (Counts)	Single Events (%)	Double Events (counts)	Raw Double Events (%)
^{109}Cd	0.0	450796	99.51	2189	0.49
^{109}Cd	0.15	613469	99.26	4548	0.74
^{109}Cd	0.30	780948	99.11	6918	0.89
^{57}Co	0.0	338956	81.98	61076	18.02
^{57}Co	0.15	428820	78.39	92663	21.61
^{57}Co	0.30	520400	78.86	110015	21.14

Data were collected at few Y positions which implies that it is unsignificant to graphically represent the double event percentage; however for both the ^{109}Cd and ^{57}Co sources the movement from a strip to the adjacent one gives an increment of the raw double events percentage of about 0.012%/μm, which is about five times lower than that detected for the movement in the X direction.

6.2. Tests with emitting source and CdTe/FE Box at a fixed position

The three sources used, i.e. ^{109}Cd, ^{241}Am, ^{57}Co, are partly collimated (semi-open sources; the stored files are labelled as **XyOPEN_coincKus**, Xy = source type, K = set coincidence time = 1μs or 4 μs). The raw data are evaluated and listed in **Table III**.

TableIII: summary of the results of the data collected in the files XyOPEN_coinc1us and XyOPEN_coinc4us (1 and 4 μs coincidence times). Other parameters are listed.

X-Ray Source	Collimator	Accum. Time (sec)	Coinc. time	Total Counts	Total Double Events	Raw Double Events (%)
^{241}Am	B	12000	1 μs	3695531	203312	5.50
^{241}Am	B	12000	4 μs	3418065	181923	5.32
^{109}Cd	D	600	1 μs	3960617	90139	2.28
^{109}Cd	D	600	4 μs	3941184	122373	3.10
^{57}Co	C	800	1 μs	2208696	335161	15.17
^{57}Co	C	800	4 μs	2209375	243697	11.03
^{57}Co (◦)	C	800	1 μs	2211208	287312	12.99
^{57}Co (◦)	C	800	4 μs			

(◦) Data with strip # 7 exchanged with strip # 8 at the Takes electronics input channels.

Superimposed typical specra of strip # 7 relative to the data accumulated with semi-open irradiating X-Ray source are reported in **Fig 12.**

The peak centroids of the 60 keV ^{241}Am, 88 keV ^{109}Cd, 122 keV ^{57}Co emission lines have been evaluated at channels 365.80, 531.50, 722.11 respectively, thus giving a straight line system response of the type **E(keV) = 0.174(keV/ch#)·Centroid(ch#)–3.65 (keV).** Figures from **13** through **15** show the raw energy spectra collected by irradiating the detector with ^{241}Am, ^{57}Co and ^{109}Cd sources, respectively at a coindence time of 1 μsec. As already anticipated in section 5 and described later, these raw data have been thereafter corrected for the false "double events": the spectra resulting from the correction procedure will be presented separately so as to make possible a direct comparison with the uncorrected spectra.

Another correction procedure has been applied to the events producing saturation in the Analog-to-Digital conversion process. Both the "false" double events and the saturated events have been discarded and only and only double cleaned events have been considered. Some comments may help to better understand the figures:

- the spectra labelled as "X spectrum" and "Y spectrum" are the spectra constructed by considering the raw data collected by the strip # 8 and # 7, respectively;
- the spectra "X double events" and "Y double events" are the energy spectra extracted respectively from the data of the strip # 8 and # 7 considering only the events induced in the detector by the same primary photon and shared by the two strips;
- the "double events spectrum" is the energy spectrum derived from the individual "X" and "Y" double events spectra and obtained by summing the energy contribution of the two strips. This energy spectrum permits to directly verify the fact that the primary photon energy is shared between the two adjacent strips and to discard undesired events (i.e. double primary photons).

As explained in section 7 (data off-line analysis), the construction of the E_X-E_Y maps (E_X= detected energy of the strip X, E_Y= detected energy of the strip Y) represents a powerful tool to inspect on "true" charge sharing double events and "false" double events. **Fig. 16** compares three E_X-E_Y maps reconstructed by analyzing the detected double events induced by ^{109}Cd, ^{241}Am and ^{57}Co X-Ray sources without any type of correction. "True" double charge sharing events tend to distribute al lower energies, i.e. at energies lower than that of the primary photon, while "false" double events are grouped along the E_X=E_Y straight line, thus indicating that they are due to different primary photons. This is evident from **Fig. 14** relative to the ^{57}Co source, where the double event spectra gives an energy peak at about 244 keV, which is justified only if anyone of two independent primary photons develops in the detector body an energy of 122 keV, corresponding to the main emission line of the ^{57}Co source.

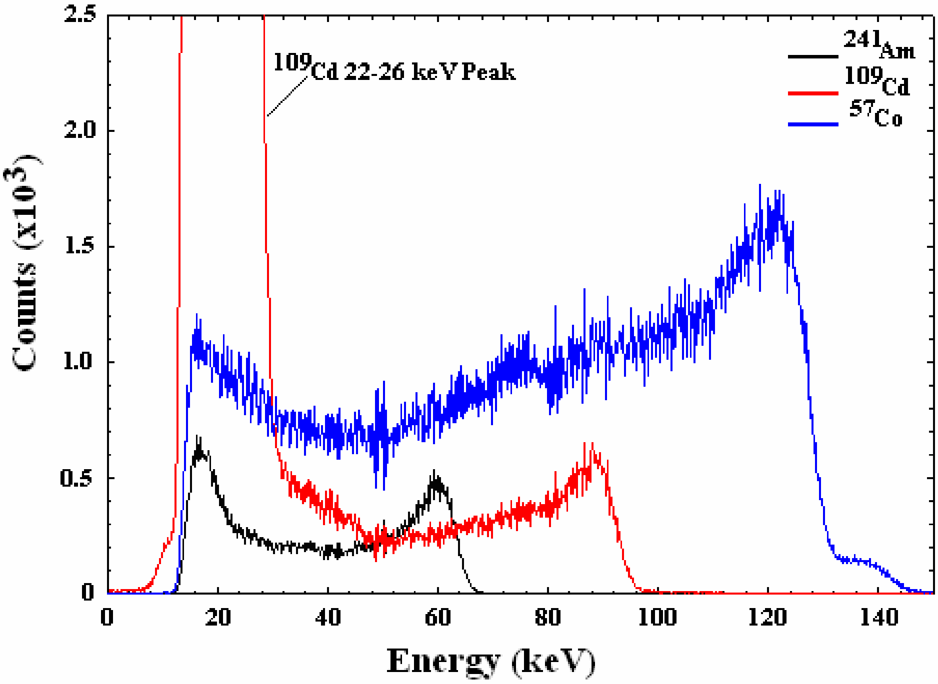

Fig. 12. Raw energy spectra collected with the strip # 7 by using ^{241}Am, ^{109}Cd, ^{57}Co X-Ray sources. The ^{109}Cd low energy (22-26 keV peak) is out of range to make possible the lower intensity peaks' visibility. Uncleaned spikes on the raw spectra denote the weighting uncertainties of the A-to-D converter in correspondence of the main binary transistions.

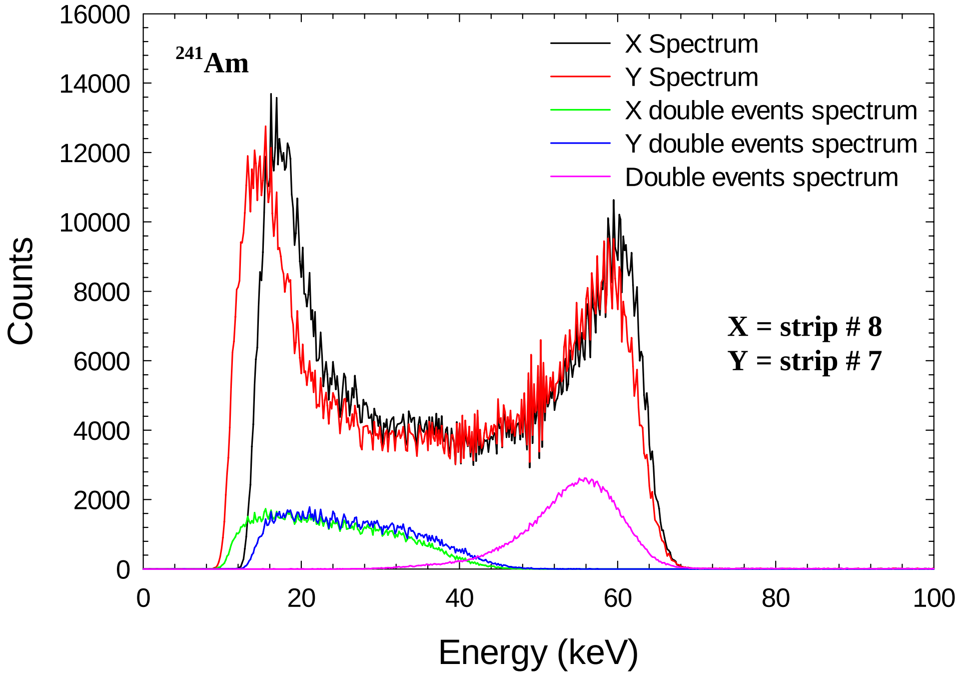

Fig. 13. ^{241}Am spectra energy raw spectrum. Double false events, due to double 60 keV primary photons coincident within the preset 1 µsec window, give a double event spectrum with a peak extending to 120 keV. Coincidence time 1 µsec.

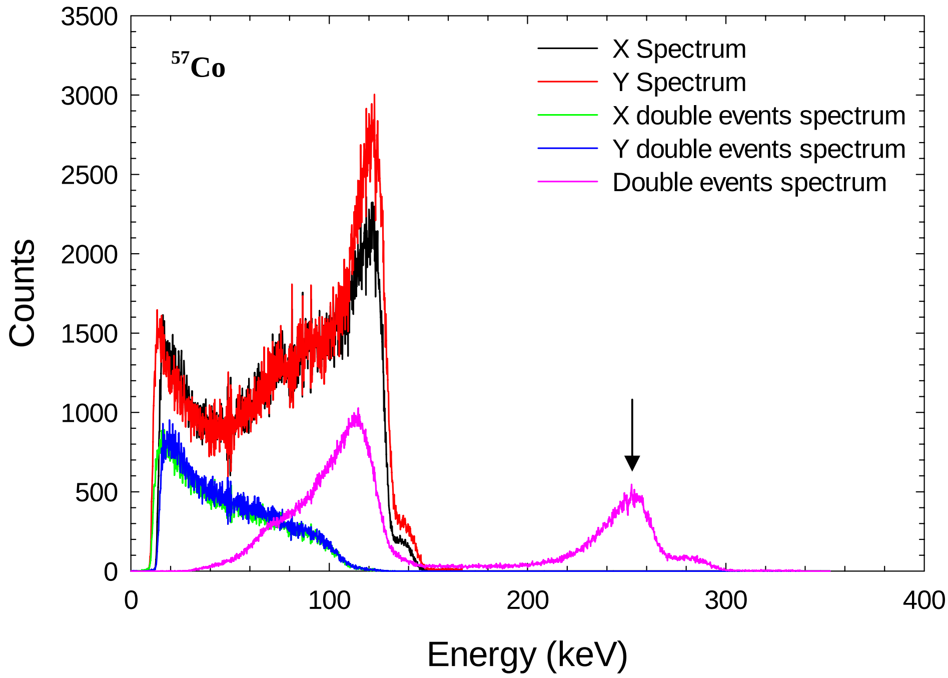

Fig. 14. Raw energy spectra collected by irradiating the detector with a ^{57}Co source. Double false events, due to 122 keV primary photons coincident within the preset 1 μsec window, give a double event spectrum with a peak extending to 244 keV.

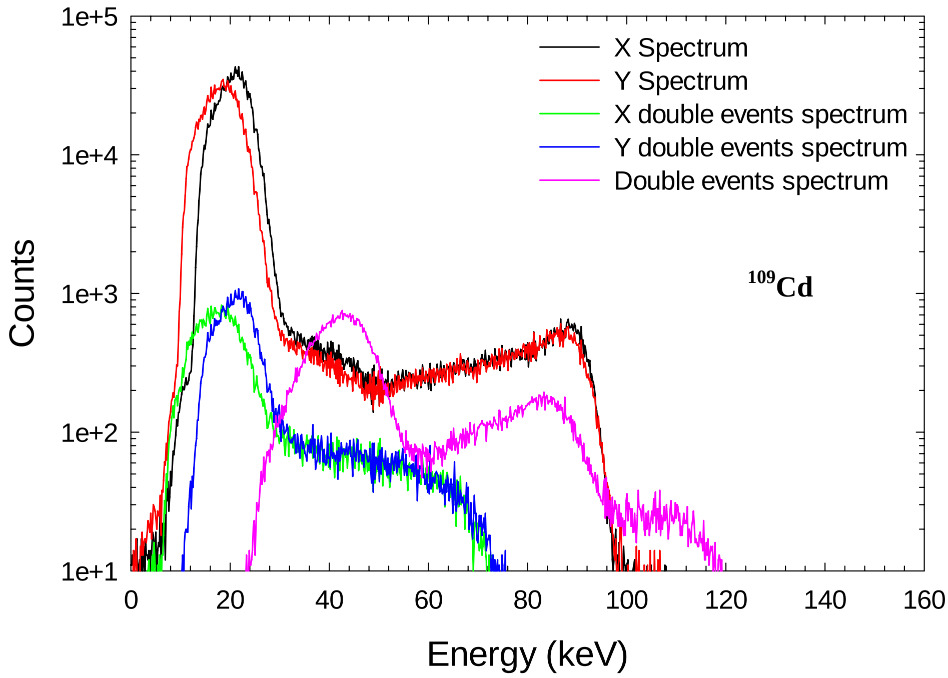

Fig. 15. Superimposed energy spectra extracted from data relative to the two strips irradiated with semi-open ^{109}Cd X-Ray source. As widely used in the text, X = strip # 8, Y = strip # 7.

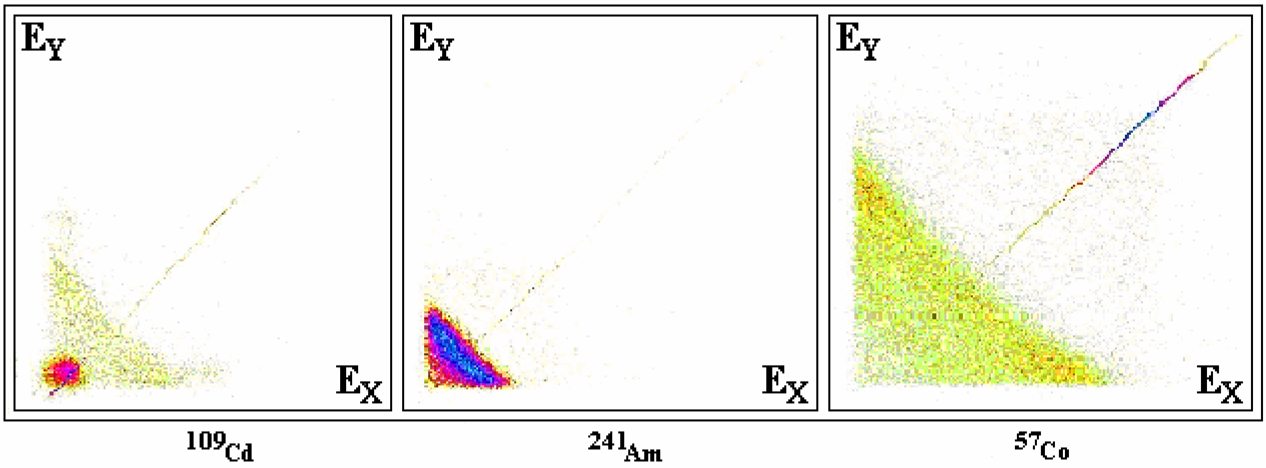

Fig. 16. E_X-E_Y double events maps extracted without any correction from raw data accumulated with three different X-Ray sources. Double "false" events are distributed along the line E_Y=E_X, while charge sharing double events are grouped at lower energies (diffuse and rarefied points). Coincidence time is 1 μsec.

It can be anticipated that to get a realistic evaluation of the double charge sharing events, the correction mechanism simply consist in eliminating the events with E_X=E_Y and considering just the events with energies outside the diagonal straight line. The effectiveness of this correction can be mainly appreciated by using the ^{57}Co source, since the primary photons are almost monoenergetic and characterized by an energy of 122 keV which, being far from the low energy regions, simplifies the distinction between false and true double events. The correction or cleaning procedure applied to the double events ^{57}Co spectrum shown in **Fig. 14** makes disappear the 244 keV energy peak due to double false charge sharing events.

6.3. Uniformity tests on the Takes channels.

Two files were collected with a semi-open ^{57}Co source (**CoOPEN_coincYus_StripEXC**, Y = 1μs or 4 μs). The difference with respect to the other measurements consists in the fact the output signals from the strips channels # 7 and # 8 are exchanged at the Takes inputs. These data (∘) are listed in the last two rows of in Table III. Non-uniformities were not detected.

6.4. Possible effect on data due to the coincidence time (coincidence window)

Data gathering with a semi-open ^{57}Co source at different times of the coincidence window. The files' names are **Co-coll_phi1&5_yus**, y = coincidence time settable within the values 1, 2, 4, 8, 16 μs. Final data will be analized and presented in detail in the Part II of the Internal Report.

6.5. Tests at a fixed position for two coincidence time values.

Collimated (W, A collimator) ^{57}Co source for two coincidence times. Files **Co-col_wus** with w = 1 and 4 μs and CdTe/FE Box in position midway between the two strips. The raw data are evaluated and listed in Table IV. See Part II for processed data.

Table IV: summary of the results of the data collected in the files Co-col_1us and Co-col_4us for 1 and 4 μs coincidence times and 21600 s accumulation time. Other parameters are listed.

X-Ray Source	Coinc. time	ASIC Gain (mV/fC)	Peaking time	Total Counts	Total Raw Double Events	Raw Double Events (%)
^{57}Co	1 μs	200	1.2 μs	321720	25377	7.31
^{57}Co	4 μs	200	1.2 μs	352030	3911	1.11

6.6. Tests at a fixed position for two values of the coincidence time and reduced ASIC gain.

Storage with an uncollimated (Pb collimator D, ϕ= 1.5 mm) ^{57}Co source for two values of the coincidence time with an halved ASIC gain (100 mV/fC instead of 200 mV/fC). Files **Co-Uncoll_Ghalf_Wus** with W = 1 and 4 μs. Data are listed in **Table V**.

Table V: summary of the results of the data collected in the files Co-Uncoll_1us and Co-Uncoll_4us for 1 and 4 μs coincidence times and 800 s accumulation time. Other parameters are listed.

X-Ray Source	Coinc. time	ASIC Gain (mV/fC)	Peaking time	Total Counts	Total Raw Double Events	Raw Double Events (%)
^{57}Co	1 μs	100	1.2 μs	707699	37052	4.98
^{57}Co	4 μs	100	1.2 μs	710449	36754	4.92

Halved ASIC's gain tests were performed to verify the correctness of the interpretation given to the combined double event spectra at energies higher than that of the primary photon (244 keV peak in Fig. 14). In fact, halving the gain, the combined double events spectra shows not only the double energy peak (244 keV), but also the triple (366 keV) and quadruple (488 keV) energy peaks due, respectively, to three and four photons which are summed as they are contemporary within the coincidence window. Data are not displayed for simplicity.

6.7. Tests at a fixed position for two values of the coincidence time, reduced ASIC gain and ASIC peaking time of 2 μsec.

Storage with an uncollimated (Pb collimator D, ϕ= 1.5 mm) ^{57}Co source for two values of the coincidence time with an halved ASIC gain (100 mV/fC instead of 200 mV/fC) and an ASIC peaking time of 2 μsec instead of 1 μsec. Files **Co-Uncoll_Ghalf_PT2us_Wus** with W = 2 and 4 μs. Data are listed in **Table VI**.

Table VI: summary of the results for the data collected in the files Co_Uncoll_Ghalf_PT2us_2us and Co-Uncoll_PT2us_4us for 2 and 4 μs coincidence times and 800 s accumulation time. Other parameters are listed.

X-Ray Source	Coinc. time	ASIC Gain (mV/fC)	Peaking time	Total Counts	Total Raw Double Events	Raw Double Events (%)
^{57}Co	1 μs	100	2 μs	927488	313380	33.79
^{57}Co	4 μs	100	2 μs	794944	72688	9.14

These tests demonstrated that the double peaking time (2 μs instead of 1 μs) had no effect on the detected double event analysis. Data are not displayed for simplicity.

6.8. Tests at a fixed position for two values of the coincidence time with an eV 16x16 pixel CZT detector (2 x 2 mm pixel size, 0.2 mm gap, 5 mm thick, HV= –550 V, readout electronics eV-16 with 200 mV/fC and 0.8 μsec peaking time).

Data accumulated for pixel # 5 and pixel # 10 with uncollimated ^{57}Co source. Files **Pix5&10-Co-coincWus** with W= 1, 2, 4, 8 μs coincidence times. data accumulated for pixel # 5 and pixel # 6 with uncollimated ^{57}Co source. Files **Pix5&6-Co-coincWus** with W= 1, 2, 4, 8 μs coincidence times. Pixels #5 and # 6 are adjacent, pixels # 5 and # 6 bordering at a corner. Data are listed in Table VII. A complete discussion on the processed data will be given in Part II.

Table VII: summary of the results for the data collected in the files Pix5&X-Co-coincWus with Y = pixel 6 or 10, W = coincidence time, 2 mm diameter collimated ^{57}Co and 900 s accumulation time. Other parameters are listed.

Pixel pair	Coinc. time (μs)	Total Counts (counts)	Single events (counts)	Single events (%)	Total Double Events (counts)	Raw Double Events (%)
Pix5&6	1	791221	506783	64.05	284438	35.95
Pix5&6	2	791796	507981	64.16	283815	35.84
Pix5&6	4	790444	758086	95.91	32358	4.09
Pix5&6	8	795223	762670	95.91	32553	4.09
Pix5&10	1	1049469	789420	75.22	260049	24.78
Pix5&10	2	1046330	787986	75.31	258344	24.69
Pix5&10	4	1047029	1041601	99.48	5428	0.52
Pix5&10	8	1047126	1041802	99.49	5324	0.51

Energy spectra relative to the third raw data of Table VII (pixel #5 and #10) are shown in **Fig. 17**. Some interesting features can be extracted from a direct comparision of this spectrum with that of **Fig. 14** relative to the stripped CdTe. First of all, as expected, the energy resolution of the CZT pixel detector is remarkably better than that of the CdTe stripped detector (individual energy spectra of the pixels # 5 an # 10 in **Fig. 17**); in fact, the secondary 136 keV ^{57}Co peak is well resolved as well as the low energy noise contribution is limited to less than 10% with respect to the 122 keV peak counts, while for the stripped CdTe detector the low energy noise contribution is approximately 60% of the counts at the 122 keV peak. The double event energy spectra shows a well defined peak at 244 keV, which means that, as already told, the double primary coincident events dominate over the charge sharing events.

The effect of the coincidence time on the double event amount is clearly shown in Table VII. The raw double events percentage is almost uniform at 1 and 2 μsec coincidence time, but falls abruptly by increasing the coincidence time from 2 to 4 μsec. The same trend has also been detected with the stripped CdTe detector (data listed in section 6.1), even with a minor amount than that observed with the pixellated CZT detector. The effect of the coincidence time on the raw double events is represented in **Fig. 18**. Further analysis (Part II) is planned both to explain the effect of the coincidence time and the difference between the pixellated CZT and the stripped CdTe detectors.

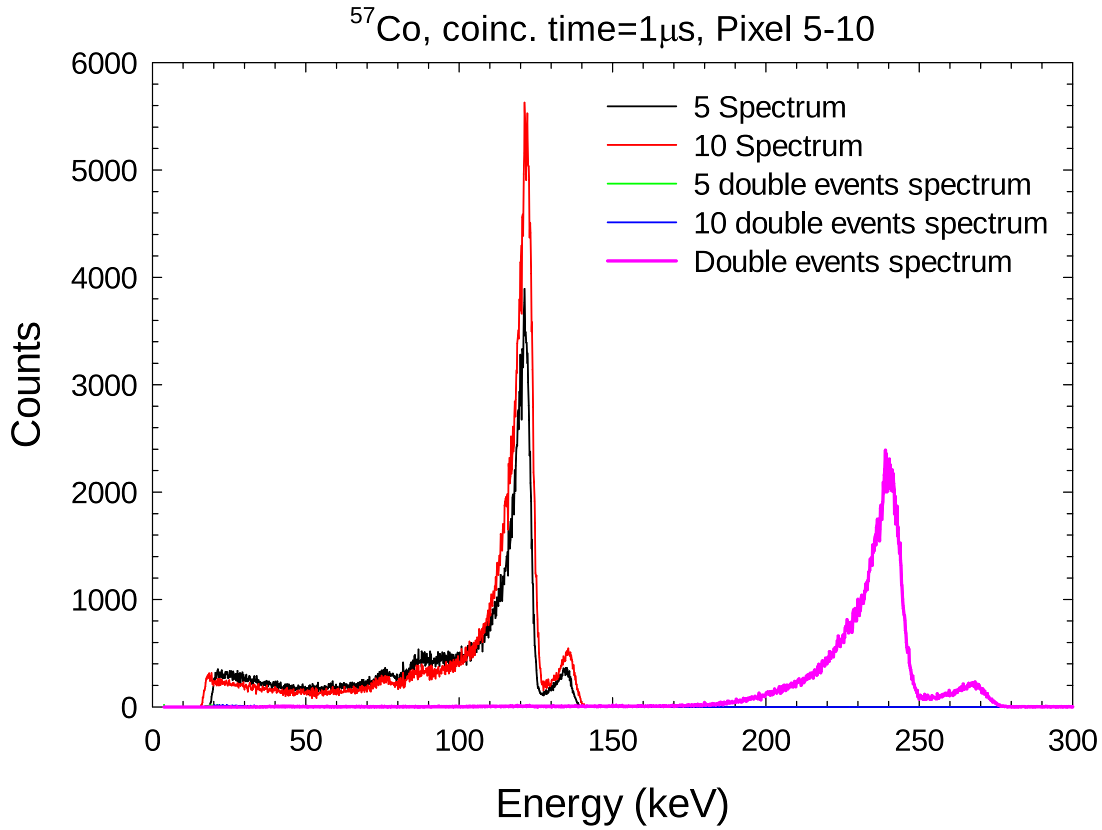

Fig. 17. Raw energy spectra as collected by irradiating the CZT pixel detector with a ^{57}Co source. Double false events, due to 122 keV primary photons coincident within the preset 1 μsec window, give a double event spectrum with a peak extending to 244 keV.

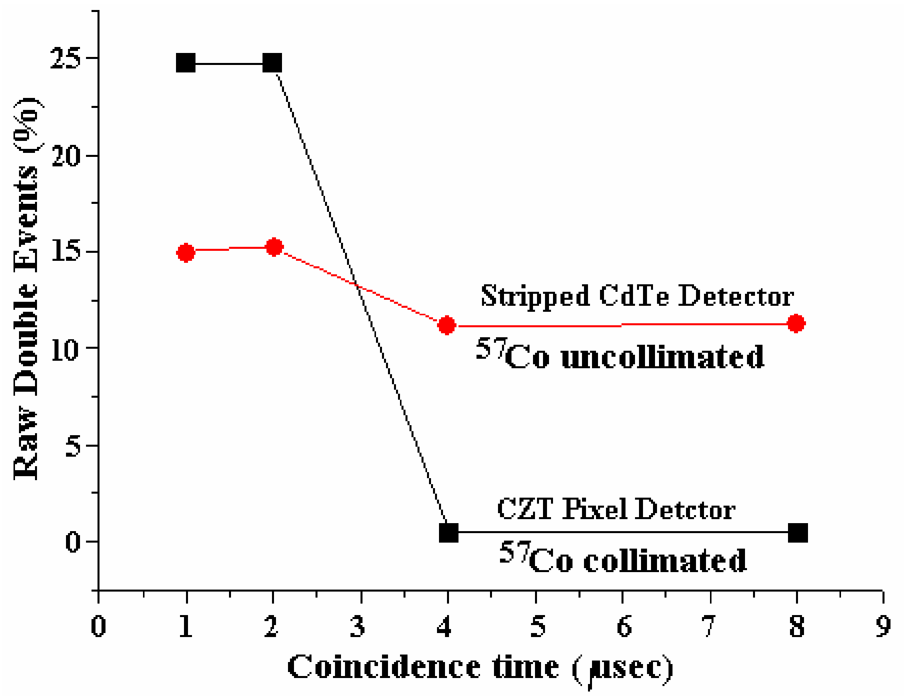

Fig. 18. Effect of the coincidence time on the raw double events data.

6.9. Tests at a fixed position and semi-open sources with a single strip connected:.

Data accumulated for single strip # 5 or strip # 8 with uncollimated ^{57}Co and ^{109}Cd sources. Four files **OneStripH__Sc_CoincOFF** with Sc= ^{57}Co or ^{109}Cd, H=7 or 8, coincidence OFF; four files **OneStripH__Sc_Coinc1us** with Sc= ^{57}Co or ^{109}Cd, H=7 or 8, coincidence 1 μsec.

6.10. Tests on double events as a function of the CdTe Bias.

Data accumulated with uncollimated sources for three coincidence times. Files **Xy_NUM_75V _Wus (**Xy **=** ^{57}Co or ^{109}Cd or ^{241}Am, NUM = ONE, TWO, THREE, W=1, 2, 4 usec; CdTe bias HV=–75V); **Xy_NOM_125V_Wus** (Xy **=** ^{57}Co or ^{109}Cd or ^{241}Am, NUM = UNO, DUE, TRE, W=1, 2, 4 usec; CdTe bias HV=–125V). See Part II for these data.

7. Data off-line analysis and results

The off-line analysis, based on a SW written in IDL (Interactive Data Language) environment, performs the following tasks:

- data file retrieval and first approximation data analysis, i.e. evaluation and separation of the double events from the total;
- statistical evaluations, i.e. total count accumulated by each strip, single and double events count rates, percentages of the double events, etc;
- energy spectra for any strip of all events accumulated;
- energy spectra for any strip of the charge condivision events;
- histograms of the charge condivision events;
- maps of the charge condivision events, i.e. assumed as **x** a strip and **y** the other, the energy E_y is represented as a function of the energy E_x. The inspection of a map has the ability to distinguish between charge condivision events (caused by a unique primary photon) and double coincident events due to the excitations of the two strips due to two separate photons (false events for the purposes of the experiment): in fact, in the map representation, because the charge condivision events share part of the primary photon energy, they are almost uniformly distributed in the E_x-E_y low energy region, while the “double-false” events are distributed, mainly for the ^{57}Co source (photon energy of 122 keV), in the high energies regions being concentrated around the diagonal E_x=E_y.
- reconstruction of the position of the charge sharing events weighting by the amplitude (energy) seen by each strip.

8. Conclusions

As already told, the results presented refer to collected raw data by using a “first approximation” analysis, i.e. extraction of single and double events, application of simple statistics, and so on. The results of more complex analysis tools will be reported in the Part II, together with the graphic presentations (spectra, histograms, maps, etc) of the corrected data.
In particular, it will be investigated:

- the double charge sharing events’ dependence on the detector bias;
- the double charge sharing events’ dependence on the coincidence time;
- the possibility and the criteria used to filter the true double events discarding the false charge sharing events;

- the behaviour of a pixellated detector;
- the adherence of the experimental results with those provided numerical simulation of the strip detector.

As anticipation of the post-processed data, **Fig. 19** shows the first approximation corrected double event percentage as a function of the X-Ray incident energy: data were extracted by subctracting from the apparent double event budget the “false” double events, as widely specified in the text and particularly in section 6.2.

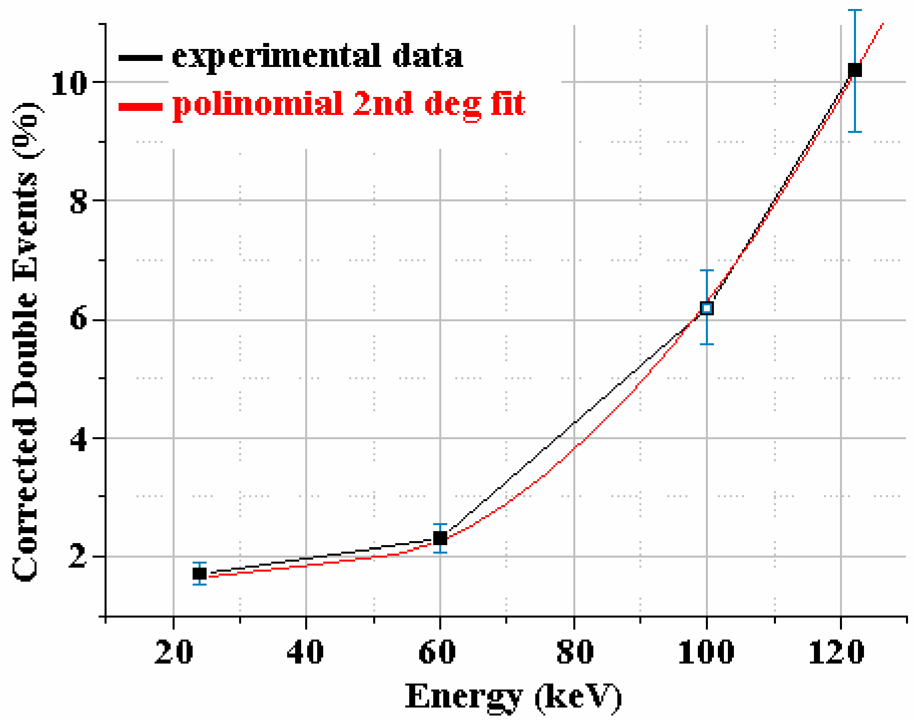

Fig. 19. Charge sharing event distribution as a function of the primary X-Ray photon. Data were corrected to eliminate the “false” double event data, i.e. the events due to independent primary photons with full energy coincident within the coincident time. Estimated data error is 10%.

Appendix I. Log of the files stored during the tests.

Detector bias HV = – 100 V.

X (μm)	Filename	Source	A	B	C	D	E	Storage time (sec)	Coinc Time (μs)
			Collimator						
– 150	Cd(-1)collim_1us	^{109}Cd	✓					10800	1
0	Cd(0)collim_1us	^{109}Cd	✓					10800	1
150	Cd(1)collim_1us	^{109}Cd	✓					10800	1
300	Cd(2)collim_1us	^{109}Cd	✓					10800	1
450	Cd(3)collim_1us	^{109}Cd	✓					10800	1
500	Cd(3a)collim_1us	^{109}Cd	✓					10800	1
600	Cd(4)collim_1us	^{109}Cd	✓					10800	1
750	Cd(5)collim_1us	^{109}Cd	✓					10800	1
800	Cd(6)collim_1us	^{109}Cd	✓					10800	1
950	Cd(7)collim_1us	^{109}Cd	✓					10800	1
1000	Cd(8)collim_1us	^{109}Cd	✓					10800	1
-	AmOPEN_coinc1us	^{241}Am		✓				12000	1
-	AmOPEN_coinc4us	^{241}Am		✓				12000	4
-	CoOPEN_coinc1us	^{57}Co			✓			800	1
-	CoOPEN_coinc4us	^{57}Co			✓			800	4
-	CdOPEN_coinc1us	^{109}Cd				✓		600	1
-	CdOPEN_coinc4us	^{109}Cd				✓		600	4
-	CoOPEN_coinc1us_StripEXC	^{57}Co			✓			800	1
-	CoOPEN_coinc4us_StripEXC	^{57}Co			✓			800	4
-	Co-coll_phi1&5_1us	^{57}Co				✓		900	1
-	Co-coll_phi1&5_2us	^{57}Co				✓		900	2
-	Co-coll_phi1&5_4us	^{57}Co				✓		900	4
-	Co-coll_phi1&5_8us	^{57}Co				✓		900	8
-	Co-coll_phi1&5_16us	^{57}Co				✓		900	16
900	Co-col_1us	^{57}Co	✓					21600	1
900	Co-col_4us	^{57}Co	✓					21600	4
-	Co-Uncoll_Ghalf_1us	^{57}Co				✓		800	1
-	Co-Uncoll_Ghalf_4us	^{57}Co				✓		800	4
-	Co-Uncoll_Ghalf_PT2us_2us	^{57}Co				✓		800	2
-	Co-Uncoll_Ghalf_PT2us_4us	^{57}Co				✓		800	4
-	Pix5&10-Co-coinc1us	^{57}Co			✓			900	1 (*)
-	Pix5&10-Co-coinc2us	^{57}Co			✓			900	2 (*)
-	Pix5&10-Co-coinc4us	^{57}Co			✓			900	4 (*)
-	Pix5&10-Co-coinc8us	^{57}Co			✓			900	8 (*)
-	Pix5&6-Co-coinc1us	^{57}Co			✓			900	1 (*)
-	Pix5&6-Co-coinc2us	^{57}Co			✓			900	2 (*)
-	Pix5&6-Co-coinc1us	^{57}Co			✓			900	4 (*)

-	Pix5&6-Co-coinc2us	^{57}Co			✓			900	8 (*)
-	OneStrip7_Co_CoincOFF	^{57}Co			✓			900	none
-	OneStrip8_Co_CoincOFF	^{57}Co			✓			900	none
-	OneStrip7_Co_Coinc1us	^{57}Co			✓			900	1
-	OneStrip8_Co_Coinc1us	^{57}Co			✓			900	1
-	OneStrip7_Cd_CoincOFF	^{109}Cd			✓			420	none
-	OneStrip8_Cd_CoincOFF	^{109}Cd			✓			420	none
-	OneStrip7_Cd_Coinc1us	^{109}Cd			✓			420	1
-	OneStrip8_Cd_Coinc1us	^{109}Cd			✓			420	1
0	Cd(Y1)_coll_CdTeOrizz_1us	^{109}Cd					✓	21600	1
150 μ	Cd(Y2)_coll_CdTeOrizz_1us	^{109}Cd					✓	21600	1
300 μ	Cd(Y3)_coll_CdTeOrizz_1us	^{109}Cd					✓	21600	1
0	Co(Y1)_coll_CdTeOrizz_1us	^{57}Cd					✓	28800	1
150 μ	Co(Y2)_coll_CdTeOrizz_1us	^{57}Cd					✓	28800	1
300 μ	Co(Y3)_coll_CdTeOrizz_1us	^{57}Cd					✓	28800	1

Collimator **A**: rectangular section 0.3mmX2mm
Collimator **B**: cylinder ϕ=3 mm
Collimator **C**: cilynder ϕ=2 mm
Collimator **D**: cilynder ϕ=1.5 mm
Collimator **E**: rectangular section 0.5mmX1mm; the 1 mm collimator's lid side is orthogonal to the longer strips' dimension.
For the data collection using a source partly collimated with **B, C, D,** the Pb collimator body is placed in contact with the outern surface of the CdTe/FE Box just in front of the Al entrance window.
(*) 16x16 pixel CZT detector.

Detector bias HV = – 75 V.

X (μm)	Filename	Source	Collimator A	B	C	D	E	Storage time (sec)	Coinc Time (μs)
-	Cd_ONE_75V_1us	^{109}Cd				✓		300	1
-	Cd_TWO_75V _2us	^{109}Cd				✓		300	2
-	Cd_THREE_75V _4us	^{109}Cd				✓		300	4
-	Am_ONE_75V_1us	^{241}Am		✓				1000	1
-	Am_TWO_75V_2us	^{241}Am		✓				1000	2
-	Am_THREE_75V_4us	^{241}Am		✓				1000	4
-	Co_ONE_75V_1us	^{57}Co			✓			300	1
-	Co_TWO_75V _2us	^{57}Co			✓			300	2
-	Co_THREE_75V _4us	^{57}Co			✓			300	4

Detector bias HV = – 125 V.

X (μm)	Filename	Source	Collimator A	B	C	D	E	Storage time (sec)	Coinc Time (μs)
-	Cd_UNO_125V_1us	^{109}Cd				✓		300	1
-	Cd_DUE_125V _2us	^{109}Cd				✓		300	2
-	Cd_TRE_125V _4us	^{109}Cd				✓		300	4
-	Am_UNO_125V_1us	^{241}Am		✓				1000	1
-	Am_DUE_125V_2us	^{241}Am		✓				1000	2
-	Am_TRE_125V_4us	^{241}Am		✓				1000	4
-	Co_UNO_125V_1us	^{57}Co			✓			300	1
-	Co_DUE_125V _2us	^{57}Co			✓			300	2
-	Co_TRE_125V _4us	^{57}Co			✓			300	4